

1 Silurian-Devonian sub-parallel ridge-trench interaction in
2 Western Junggar and North-Central Tianshan in NW
3 China: Alternative genesis of archipelagic architecture
4 **Ji'en Zhang¹, Yichao Chen², Wenjiao Xiao¹, John Wakabayashi³, Brian F.**
5 **Windley⁴, Shuaihua Song^{1, 2}, and Jiyuan Yin⁵**

6 ¹ *State Key Laboratory of Lithospheric Evolution, Institute of Geology and Geophysics,*
7 *Chinese Academy of Sciences, Beijing 100029 China*

8 ² *University of Chinese Academy of Sciences, Beijing 100049 China*

9 ³ *Department of Earth and Environmental Sciences, California State University, Fresno,*
10 *CA 93740 USA*

11 ⁴ *Department of Geology, University of Leicester, Leicester, LE1 7RH, United Kingdom*

12 ⁵ *Institute of Geology, Chinese Academy of Geological Sciences, Beijing 100037, China*

13

14

15

16

17

18

19

20

21

22

23 **ABSTRACT**

24 Western Junggar and North-Central Tianshan in NW China comprise a double
25 magmatic belt, which evolved as a result of 446-380 Ma SSZ-type gabbro-basalt-
26 andesite-diorite-granite-rhyolite magmatism that intruded a 504-446 Ma accretionary
27 complex in SW Junggar and coeval magmatic arc in Central Tianshan. This orogenic
28 framework is interpreted as a product of sub-parallel ridge-trench interaction, which
29 generated the double magmatic belt together with adakitic intrusions in the older
30 accretionary complex. In this model, a buoyant subducted ridge stalled and separated
31 the double magmatic belts, resulting in the opening of a new 414-325 Ma intra-arc
32 ocean, which is represented by Nb-depleted OIB- and MORB-type ophiolites. Mafic
33 rocks generated by sea floor spreading in the modern Gulf of California record a similar
34 evolution and chemistry. This new ocean split the northern accretionary complex along
35 Mt. Xiemisitai-Barleik-Mayile line, leading to deposition of Devonian shallow marine-
36 terrestrial sediments and cessation of magmatism at 380-349 Ma; this evolution also
37 resembles that of the late Cenozoic passive margins of Baja California. Subsequent
38 removal of the new ocean and its ridge-subduction gave rise to an archipelagic
39 framework in the Late Paleozoic. A worldwide analysis of published examples of sub-
40 parallel ridge-trench interaction indicates that a ridge jump can lead to multiple episodes
41 of subduction, which could occur long before terminal ocean closure.

42

43 INTRODUCTION

44 A spreading ridge can interact with a trench at a range of convergence angles
45 (Sisson et al., 2003). Sub-parallel subduction can generate a short-lived magmatic belt
46 in a forearc setting, adjacent to a magmatic arc, comparable to relations in Eocene
47 Alaska, modern western California and the Chile triple junction (Sisson et al., 2003);
48 we term these synchronous sub-parallel magmatic belts as “double magmatic belts”.
49 Stalling of the subduction of a buoyant ridge (van Wijk et al., 2001) rifts the upper plate
50 to develop a passive continental margin, and then forms new oceanic crust above
51 upwelling sub-ridge asthenosphere, separating the two magmatic belts, as has taken
52 place in Baja California and the Gulf of California (Michaud et al., 2006). Such a plate
53 boundary configuration can evolve further into an archipelagic architecture with
54 continued oceanic spreading and subduction.

55 The western Altaids (Fig. 1a), one of the world’s classic orogens, was generated
56 by subduction of the western segment of the Paleo-Asian Ocean (Xiao et al., 2015).
57 This orogen evolved along a major subduction zone with local archipelagic
58 configurations, which generally formed via forearc and backarc spreading with one
59 magmatic belt (Windley et al., 2007; Xiao et al., 2015). However, existing models
60 cannot explain the 446-380 Ma double magmatic belt, between which developed 414-
61 325 Ma oceanic crust developed in SW Junggar and Chinese North-Central Tianshan,
62 an eastern extension of the Yili block (Fig. 1b). This complex configuration requires an
63 alternative tectonomagmatic model.

64 This paper will present a new tectonic model for the evolution of SW Junggar and

65 North-Central Tianshan that includes mid-Paleozoic sub-parallel ridge-subduction
66 leading to a Late Paleozoic archipelago configuration in the western Altaids.

67 **TECTONIC UNITS**

68 Western Junggar is divisible into SW Junggar and NW Junggar units along a
69 boundary north of the Tacheng basin-Mt. Xiemisitai-Hongguleleng (Fig. 1b). In north
70 and west SW Junggar are 472-531 Ma OIB- and MORB-type ophiolites, and 379-414
71 Ma OIB- and MORB-type ophiolites depleted in Nb crop out in the Baijiantan area and
72 along the Darbut Fault there are (Figs. 1b, 2a) (Zhang et al., 2011; Zhang et al., 2018).

73 In the Mt. Xiemisitai-Mayile area in SW Junggar a 380-446 Ma SSZ-type gabbro-
74 basalt-andesite-diorite-granite-rhyolite intrudes an Early Paleozoic accretionary
75 complex (Chen et al., 2010; Yin et al., 2017). 300-349 Ma magmatism is widespread to
76 north and south of the Late Paleozoic accretionary complex (Figs. 1b, 2a). NW Junggar
77 includes Late Paleozoic Saur arc rocks, and an accretionary complex with
78 Carboniferous turbidites juxtaposed with Ordovician Kujibai ophiolite (Figs. 1b,
79 2d)(Chen et al., 2017).

80 The Central Tianshan exposes Precambrian basement, a long-lived 300-476.5 Ma
81 magmatic belt, and Silurian-Carboniferous mylonite, gneiss and amphibolites (Figs. 1b,
82 2e) (Wang et al., 2012). In the North Tianshan, situated between the Central Tianshan
83 and SW Junggar, an accretionary complex consists of Carboniferous turbidites and 325-
84 386 Ma OIB- and MORB-type ophiolites with depleted Nb (Figs. 1b, 2e) (Xu et al.,
85 2006).

86 **METHODOLOGY**

87 To exclusively constrain orogenic processes of a short-lived archipelagic
88 architecture with dismembered accretionary complex and paired igneous arc is
89 generally difficult, because many ways can evolve into this framework. In order to solve
90 this issue, we firstly remove complicated younger orogenic units and affiliate to an older
91 episode at which just has one accretionary complex and a contemporaneous arc to
92 constitute a subduction zone; then linking this subduction zone to evolving spatial
93 relationships of following associated subduction episodes.

94 It is noteworthy that deduced results of each orogenic stage should match the facts
95 and data collected from field work and indoor analysis.

96 **EARLY PALEOZOIC SUBDUCTION SYSTEM**

97 Li et al. (2006) proposed that the North-Central Tianshan and SW Junggar in China
98 (separated by the Aibihu Fault) evolved independently (Fig. 1b), but paleomagnetic
99 data show that the SW Junggar underwent 35° counterclockwise post-Permian rotation
100 (Fig. 1b)(Choulet et al., 2011) suggesting that it was previously aligned parallel with
101 the North-Central Tianshan.

102 In SW Junggar a 479-446 Ma accretionary complex, containing 458-504 Ma
103 blueschist and Ordovician-Silurian turbidites, lacks a coeval island arc. In the Central
104 Tianshan a 476.5-439 Ma continental arc lacks a paired accretionary complex (Fig. 1b).

105 Moreover, SW Junggar and Central Tianshan were in contact by the Early-Middle
106 Paleozoic, based on the following. (1) Quartzitic schist from Laba River at southern
107 end of SW Junggar (Fig. 1b and DR2) and at Wenquan in the Central Tianshan (across
108 the Aibihu Fault) share similar clastic components (Fig. 1b). (2) Silurian-Devonian

109 strata from SW Junggar have detrital zircon age peaks at 380-500, 600, 900-1000, 1500-
110 1700, 2400-2500 Ma similar to those in the Central Tianshan (Figs. 1b, 2b, f, DR3a-b),
111 and (3) contain Precambrian and 446-479 Ma clasts, the sources of which are absent in
112 SW Junggar (Figs. 2a, b, e), indicating their provenance from the Central Tianshan.
113 Accordingly, the evidence suggests that the SW Junggar accretionary complex and
114 Central Tianshan arc constitute a 476.5-446 Ma trench-arc system (Fig. 3a).

115 MIDDLE PALEOZOIC SUB-PARALLEL RIDGE-TRENCH INTERACTION

116 In the mid-Paleozoic continuous evolving subduction generated 380-446 Ma
117 magmatic rocks that intruded the Early Paleozoic accretionary complex in SW Junggar
118 (Chen et al., 2010) and a coeval magmatic arc in the Central Tianshan, forming a
119 double-magmatic belt (Fig. 2). We interpret the magmatic rocks that intrude the
120 accretionary complex (including adakitic granodiorites with positive $\epsilon_{\text{Nd}}(t)$) in the Mt.
121 Xiemisitai area (Fig. 3b) (Yin et al., 2017), as products of a slab window beneath SW
122 Junggar, caused by (a) a subducted spreading ridge or (b) a slab tear in old subduction
123 lithosphere (Calmus et al., 2011). Between the double magmatic belts, younger 325-
124 414 Ma MORB-type ophiolites with depleted Nb occur in SW Junggar and Chinese
125 North Tianshan, which may have developed in (c) a rift basin above a buoyant
126 subducting slab or in (d) a back-arc/forearc basin.

127 If the MORB-type ophiolites developed in a sizable back-arc or forearc basin
128 (model d), a coeval 349-380 Ma trench and island arc should be located in SW Junggar,
129 in contrast to the actual field relationship (Fig. 1b).

130 The presence of 325-414 Ma ophiolites in the Late Paleozoic SW Junggar and

131 Chinese North Tianshan accretionary complexes makes the slab-tear model (b) unlikely,
132 because they are younger than the time of the double magmatic belts (446-414 Ma).

133 Therefore, we prefer hypothesis (a, c) that a Middle Paleozoic ridge parallel to a
134 trench subducted beneath SW Junggar (Fig. 3c), because it agrees best with the field
135 relationships and has modern analogues. In our model, a buoyant subducted ridge
136 stalled resulting in rifting of the upper plate and opening of a new SW Junggar/Chinese
137 North Tianshan ocean, similar to the extant Gulf of California (Michaud et al., 2006).

138 The trench migrated to the southern margin of this ocean in the Tianshan (Fig. 3c),
139 enabling 414-386 Ma oceanic crust in SW Junggar to be accreted before the 386-325
140 Ma ophiolites in the Chinese North Tianshan (Figs. 1b, 2a, e). This resulted in the
141 Central Tianshan continental arc being generated by a subduction system analogous to
142 those in modern Alaska and Chile (Thorkelson et al., 2011) and 357-375 Ma
143 deformation and metamorphism (Fig. 3c). The subduction of the spreading ridge may
144 have resulted in magmatic interaction with an overlying metasomatized mantle wedge
145 or it may have promoted partial melting of this mantle wedge to generate MORB-type
146 oceanic crust with depleted Nb (Zhang et al., 2011); this would be similar to mafic rocks
147 in the Gulf of California (Calmus et al., 2011).

148 Devonian shallow marine-terrestrial sediments with corals, brachiopods, sea lilies,
149 and plants (Gong and Zong, 2015) were deposited on the northern margin of the Early
150 Paleozoic accretionary complexes along the Mt. Xiemisitai-Barleik-Mayile line (Fig.
151 1b), and magmatism ceased from 380 to 349 Ma (Liu et al., 2017); these sedimentary-
152 kinematic relations are similar to those in the young passive continental margin above

153 a remnant slab in Baja California (Paulssen and de Vos, 2017). Moreover,
154 Carboniferous sandstones in SW Junggar contain 349-380 Ma detrital zircons
155 suggesting a source in the Central Tianshan (Fig. 2a, c, e, 3c).

156 **ARCHIPELAGIC ARCHITECTURE OF THE WESTERN ALTAIDS**

157 The new ocean evolved to form Late Paleozoic intra-oceanic subduction systems
158 with a continental arc in an overall archipelago configuration. The ocean subducted
159 southwards to generate the Chinese North Tianshan accretionary complex (Xu et al.,
160 2006) and the long-lived Central Tianshan continental arc (Fig. 3d).

161 A double-vergent subduction system developed in SW Junggar (Zhang et al., 2011).
162 Southward subduction generated an intra-oceanic arc at Guai 10 (Fig. 1b) in the NW
163 Junggar Basin and an accretionary complex containing Carboniferous turbidites and the
164 Baijiantan-Baikouquan ophiolites (Figs. 1b, 3d). Northward subduction resulted in
165 formation of the Mt. Xiemisitai-Mayile-Barleik magmatic arc and an accretionary
166 wedge including the Darbut ophiolite (Figs. 1b, 3d). The young ridge subducted (Fig.
167 3d) to generate the Baogutu adakites and high-Mg# sanukitoids and the Miaoergou
168 charnockite (Zhang et al., 2011).

169 In NW Junggar, the Paleo-Asian Ocean subducted northward to form a Late
170 Paleozoic accretionary complex that includes Carboniferous trench sandstones
171 juxtaposed with the Ordovician Kujibai ophiolite (Fig. 3d) (Chen et al., 2017).

172 Our new model suggests that such an archipelagic architecture in the western
173 Altaids evolved as a consequence of sub-parallel ridge subduction. This type of
174 subduction mechanism and subsequent evolution leads to a complex rifting and

175 amalgamation. The recognition of double magmatic belts provides a means of tracking
176 such a complex history in orogenic belts.

177 **IMPLICATIONS**

178 Sub-parallel ridge-trench interactions characterize modern subduction zones, so
179 such interactions would be expected in the formation of some ancient orogenic belts
180 such as western Altaids. It is noteworthy that a spreading ridge can undergo multiple
181 episodes of subduction, resulting in generation of an archipelagic framework.

182 **ACKNOWLEDGEMENTS**

183 We thank the referees for helpful reviews. This work has been supported by the
184 National Key R & D Program of China (2017YFC0601206), the Strategic Priority
185 Research Program (B) of CAS (XDB18030103, XDB18020203), and the National
186 Natural Science Foundation of China (41472208).

187 **REFERENCES CITED**

188 Calmus, T., Pallares, C., Maury, R. C., Aguillón-Robles, A., Bellon, H., Benoit, M., and
189 Michaud, F., 2011, Volcanic Markers of the Post-Subduction Evolution of Baja
190 California and Sonora, Mexico: Slab Tearing Versus Lithospheric Rupture of the
191 Gulf of California: Pure and Applied Geophysics, v. 168, no. 8, p. 1303-1330.

192 Chen, J. F., Han, B. F., Ji, J. Q., Zhang, L., Xu, Z., He, G. Q., and Wang, T., 2010, Zircon
193 U-Pb ages and tectonic implications of Paleozoic plutons in northern West Junggar,
194 North Xinjiang, China: Lithos, v. 115, no. 1-4, p. 137-152.

195 Chen, Y. C., Xiao, W. J., Windley, B. F., Zhang, J. E., Zhou, K. F., and Sang, M., 2017,
196 Structures and detrital zircon ages of the Devonian-Permian Tarbagatai

197 accretionary complex in west Junggar, China: imbricated ocean plate stratigraphy
198 and implications for amalgamation of the CAOB: *International Geology Review*,
199 v. 59, no. 9, p. 1097-1115.

200 Choulet, F., Chen, Y., Wang, B., Faure, M., Cluzel, D., Charvet, J., Lin, W., and Xu, B.,
201 2011, Late Paleozoic paleogeographic reconstruction of Western Central Asia
202 based upon paleomagnetic data and its geodynamic implications: *Journal of Asian
203 Earth Sciences*, v. 42, no. 5, p. 867-884.

204 Gong, Y. M., and Zong, R. W., 2015, Paleozoic stratigraphic regionalization and
205 paleogeographic evolution in Western Junggar, Northwestern China: *Earth Science*,
206 v. 40, no. 3, p. 461-484 (in Chinese with English abstract).

207 Li, J. Y., He, G. Q., Xu, X., Li, H. Q., Sun, G. H., Yang, T. N., Gao, L. M., and Zhu, Z.
208 X., 2006, Crustal tectonic framework of Northern Xinjiang and adjacent regions
209 and its formation: *Acta Geologica Sinica*, v. 80, no. 1, p. 148-168 (in Chinese with
210 English abstract).

211 Liu, B., Han, B. F., Chen, J. F., Ren, R., Zheng, B., Wang, Z. Z., and Feng, L. X., 2017,
212 Closure Time of the Junggar-Balkhash Ocean: Constraints From Late Paleozoic
213 Volcano-Sedimentary Sequences in the Barleik Mountains, West Junggar, NW
214 China: *Tectonics*, v. 36, no. 12, p. 2823-2845.

215 Michaud, F., Royer, J. Y., Bourgois, J., Dyment, J., Calmus, T., Bandy, W., Sosson, M.,
216 Mortera-Gutiérrez, C., Sichler, B., Rebolledo-Viera, M., and Pontoise, B., 2006,
217 Oceanic-ridge subduction vs. slab break off: Plate tectonic evolution along the Baja
218 California Sur continental margin since 15 Ma: *Geology*, v. 34, no. 1, p. 13-16.

219 Paulssen, H., and de Vos, D., 2017, Slab remnants beneath the Baja California peninsula:
220 Seismic constraints and tectonic implications: *Tectonophysics*, v. 719-720, p. 27-
221 36.

222 Sisson, V. B., Ravlis, T. L., Roeske, S. M., and Thorkelson, D. J., 2003, Introduction:
223 An overview of ridge-trench interactions in modern and ancient settings, in Sisson,
224 V. B., Roeske, S. M., and Pavlis, T. L., eds., *Geology of a transpressional orogen*
225 developed during ridge-trench interaction along the North Pacific margin: Boulder,
226 Colorado, GSA Special Paper, 371, p. 1-18.

227 Thorkelson, D. J., Madsen, J. K., and Sluggett, C. L., 2011, Mantle flow through the
228 Northern Cordilleran slab window revealed by volcanic geochemistry: *Geology*, v.
229 39, no. 3, p. 267-270.

230 van Wijk, J. W., Govers, R., and Furlong, K. P., 2001, Three-dimensional thermal
231 modeling of the California upper mantle: a slab window vs. stalled slab: *Earth and*
232 *Planetary Science Letters*, v. 186, no. 2, p. 175-186.

233 Wang, B., Jahn, B. M., Shu, L. S., Li, K. S., Chung, S. L., and Liu, D. Y., 2012, Middle-
234 Late Ordovician arc-type plutonism in the NW Chinese Tianshan: Implication for
235 the accretion of the Kazakhstan continent in Central Asia: *Journal of Asian Earth*
236 *Sciences*, v. 49, no. 0, p. 40-53.

237 Windley, B. F., Alexeiev, D., Xiao, W. J., Kröner, A., and Badarch, G., 2007, Tectonic
238 models for accretion of the Central Asian Orogenic belt: *Journal of the Geological*
239 *Society, London*, v. 164, p. 31-47.

240 Xiao, W., Windley, B. F., Sun, S., Li, J., Huang, B., Han, C., Yuan, C., Sun, M., and

241 Chen, H., 2015, A Tale of Amalgamation of Three Permo-Triassic Collage Systems
242 in Central Asia: Oroclines, Sutures, and Terminal Accretion: Annual Review of
243 Earth and Planetary Sciences, v. 43, no. 1, p. 477-507.

244 Xu, X. Y., Li, X. M., Ma, Z. P., Xia, L. Q., Xia, Z. C., and Peng, S. X., 2006, LA-ICPMS
245 zircon U-Pb dating of gabbro from the Bayingou ophiolite in the Northern Tianshan
246 Mountains: *Acta Geologica Sinica*, v. 80, no. 8, p. 1168-1176 (in Chinese with
247 English abstract).

248 Yin, J. Y., Chen, W., Xiao, W. J., Yuan, C., Windley, B. F., Yu, S., and Cai, K. D., 2017,
249 Late Silurian–early Devonian adakitic granodiorite, A-type and I-type granites in
250 NW Junggar, NW China: Partial melting of mafic lower crust and implications for
251 slab roll-back: *Gondwana Research*, v. 43, p. 55-73.

252 Zhang, J. E., Xiao, W. J., Han, C. M., Ao, S. J., Yuan, C., Sun, M., Geng, H. Y., Zhao,
253 G. C., Guo, Q. Q., and Ma, C., 2011, Kinematics and age constraints of deformation
254 in a Late Carboniferous accretionary complex in Western Junggar, NW China:
255 *Gondwana Research*, v. 19, no. 4, p. 958-974.

256 Zhang, J. E., Xiao, W. J., Luo, J., Chen, Y. C., Windley, B. F., Song, D. F., Han, C. M.,
257 and Safonova, I., 2018, Collision of the Tacheng block with the Mayile-Barleik-
258 Tangbale accretionary complex in Western Junggar, NW China: Implication for
259 Early-Middle Paleozoic architecture of the western Altaids: *Journal of Asian Earth
260 Sciences*, v. 159, p. 259-278.

261 **FIGURE CAPTIONS**

262 Figure 1 (a) Geological map of the West Junggar and Chinese North-Central Tianshan,

263 showing spatial relationships of the main orogenic components, including 380-446 Ma
264 double magmatic belts, separated by 325-414 Ma oceanic crust, intruded into an Early-
265 Middle Paleozoic accretionary complex in SW Junggar and a magmatic arc in the
266 Central Tianshan. See Figure DR1 for further details. (b) Inserted schematic map of
267 East Asia showing the location of the Altaids (Xiao et al., 2015).

268 Figure 2 Time-stratigraphic relationships between ophiolites, magmatism, HP
269 metamorphism, and detrital zircons in sedimentary rocks in SW Junggar (a-c), NW
270 Junggar (d) and the Chinese North-Central Tianshan (e-f). Note the development of
271 380-446 Ma double magmatic belts, which are older than 325-414 Ma ophiolites in the
272 SW Junggar and Chinese North Tianshan (a, e). Detrital zircons of Precambrian and
273 446-479, 349-380 Ma, which are magmatic gaps in the SW Junggar (a), are dated in
274 Silurian-Devonian (b) and Carboniferous (c) strata. The source of these clasts is in the
275 Central Tianshan (e-f). Light green bars and dark green graphs in b, c, f present detrital
276 zircons of 300-550 and 550-3500 Ma, respectively.

277 Figure 3 Four diagrams illustrating the tectonic crustal evolution in the West Junggar
278 and Chinese North-Central Tianshan, showing the progressive development of Early
279 Paleozoic subduction zone, Middle Paleozoic sub-parallel ridge-trench interaction, and
280 a final Late Paleozoic archipelagic framework by 349-316 Ma. Acronyms are defined
281 in Fig. 1. Further discussion in the text.

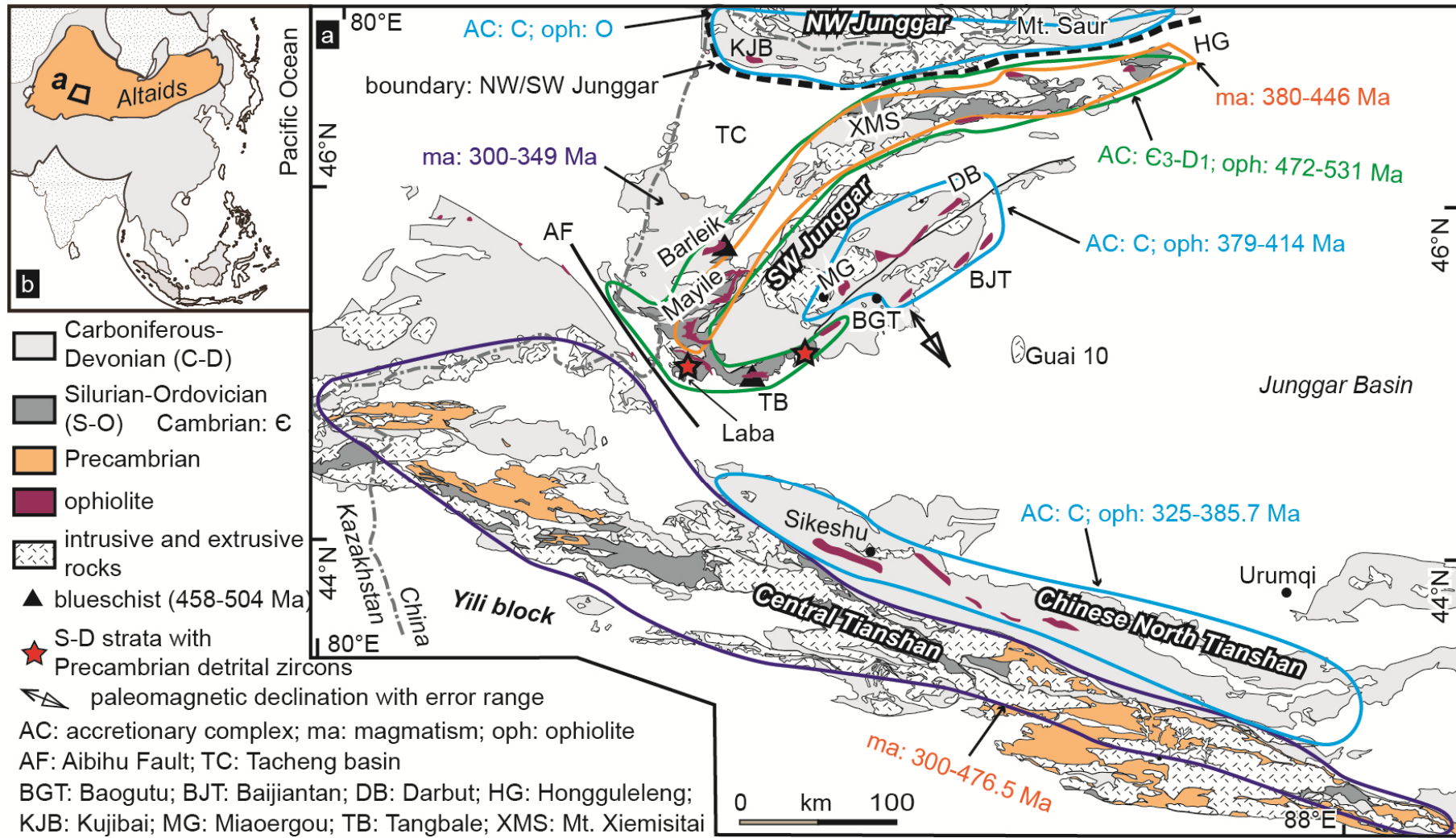


Figure 1 Zhang et al., 2019

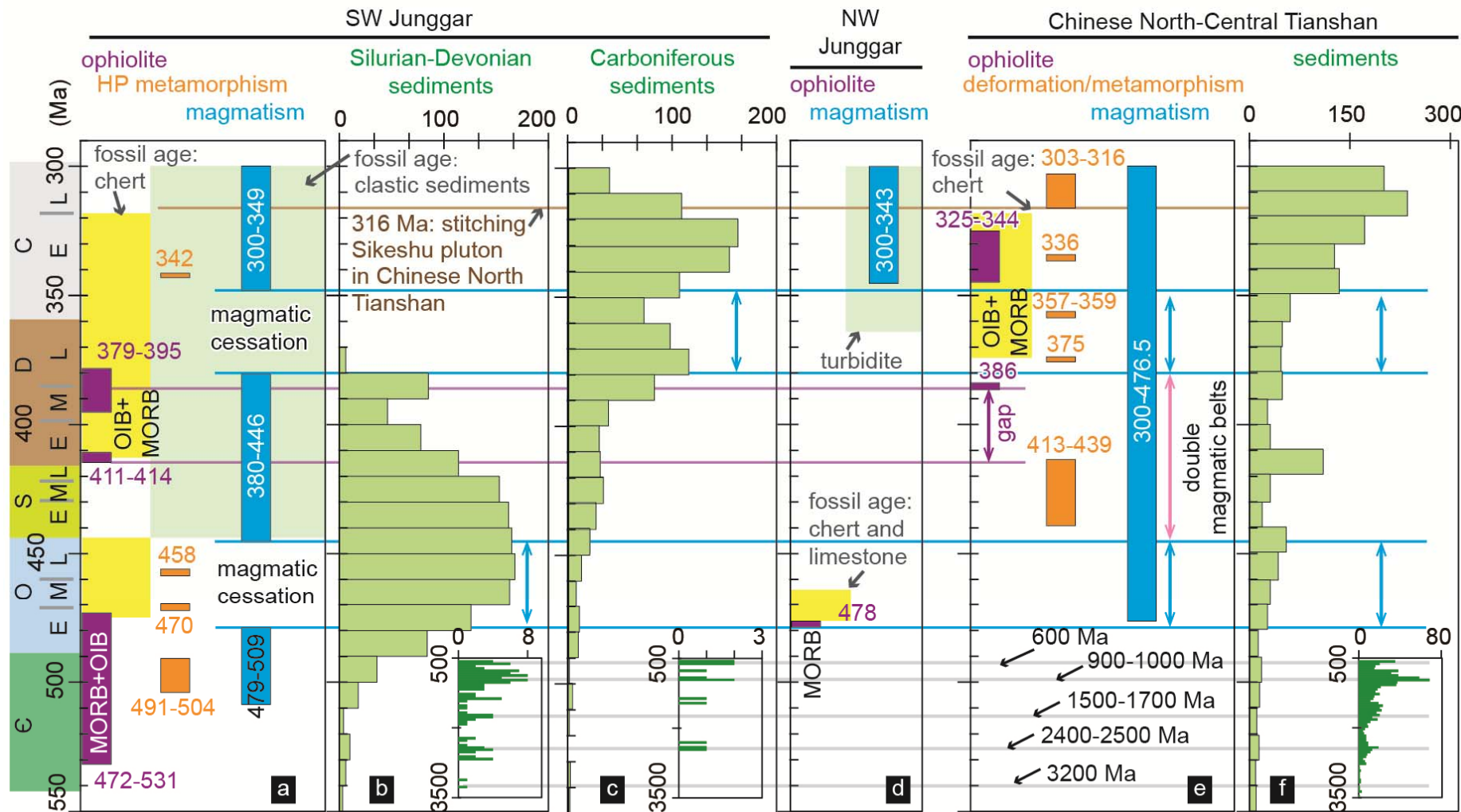


Figure 2 Zhang et al., 2019

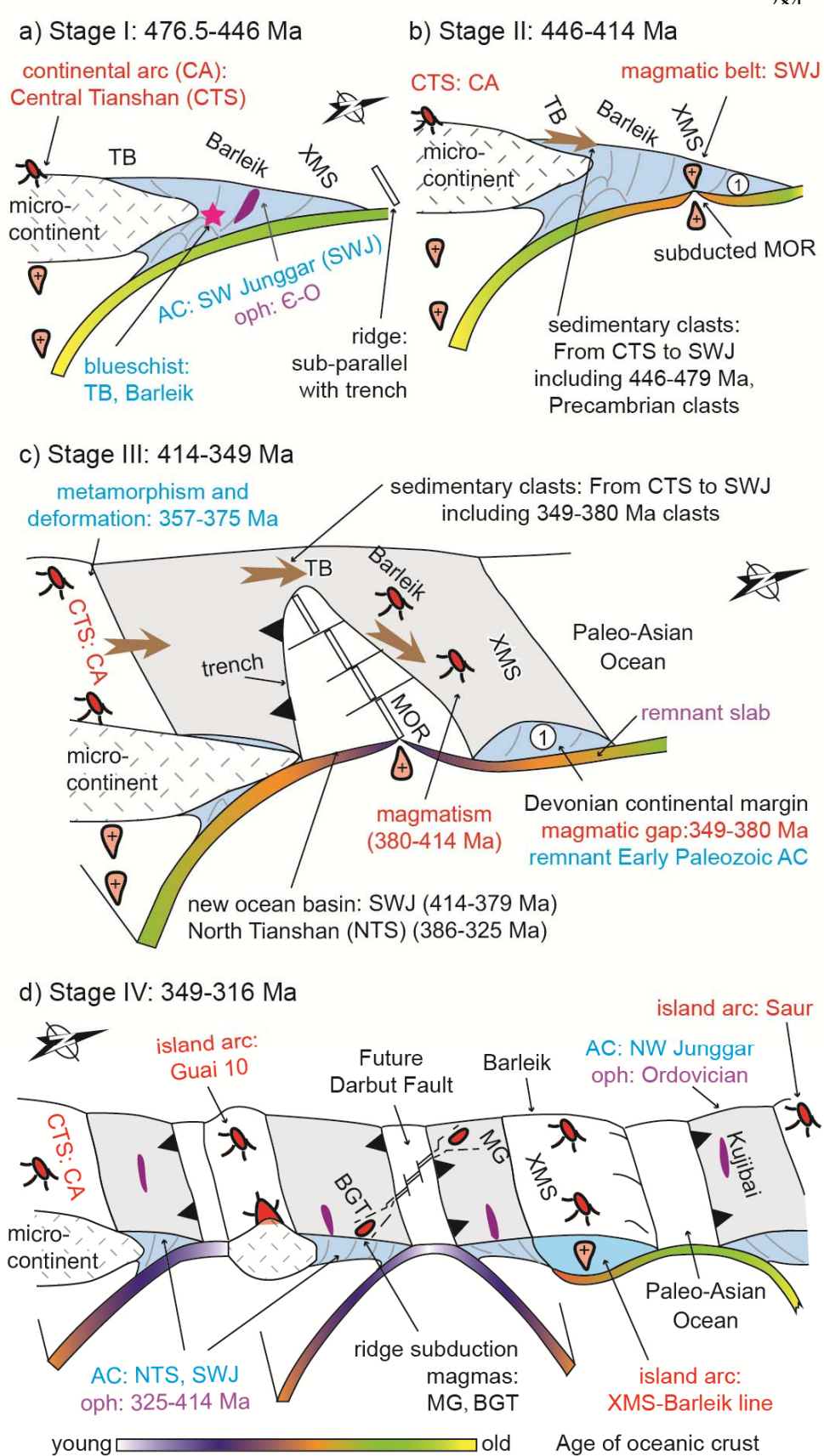


Figure 3 Zhang et al., 2019